JOURNAL OF GUIDANCE, CONTROL, AND DYNAMICS
Vol. 16, No. 5, September–October 1993

Robustness Analysis of a Multirate Flutter Suppression System

Gregory S. Mason* and Martin C. Berg†
University of Washington, Seattle, Washington 98195

A unified approach for analyzing the robustness and performance of multirate systems is presented. The approach is a compilation of existing multirate performance and robustness analysis results, along with some new results, all presented in a consistent state-space formulation. The approach is used to analyze the robustness of a multirate flutter suppression system designed for a model wing. The example highlights some of the practical considerations in multirate performance and robustness analysis.

Introduction

NUMEROUS approaches have been taken to analyze the stability and robustness of multirate systems. Most notable is the work of Thompson,[1] Thompson and Dailey,[2] Meyer and Burrus,[3] and Khargonekar et al.[4] References 1 and 2 analyzed the gain and phase margins of a multirate system using an approach based on Kranc vector switch decomposition. Meyer and Burrus studied the stability of multirate systems and their frequency domain responses by applying the concept of block processing to multirate systems. Khargonekar et al. analyzed the robustness of periodic compensators, a super set of multirate compensators, using isomorphisms.

Although these approaches seem quite diverse, fundamentally they are very similar. These three approaches, along with most multirate analysis techniques, use a transformation, such as Kranc vectors or block processing, to convert the multirate system into an equivalent single-rate system which can be analyzed with established single-rate techniques. The single-rate results are then used to characterize the stability and robustness of the original multirate system.

In this paper we compile the important multirate analysis results from Refs. 1–6 and present them in a unifying state-space formulation. In addition, we provide some new results that clarify the relationship between a multirate system and its single-rate equivalent. Finally, we apply all of these results to a practical example: a multirate flutter suppression system designed for a model wing.

Summary of Multirate Analysis Tools

In this section we summarize some important and useful multirate robustness analysis results. These results are applicable to multirate systems that are linear, causal, finite-dimensional, and whose sample/update/delay activities are periodic and synchronized to a common clock.

Result 1

A multirate system can be modeled as an equivalent single-rate system (ESRS). Modeling a multirate system as an ESRS is fundamental to multirate robustness analysis. The ESRS allows one to manipulate and analyze a multirate system as if it were single rate. Using the ESRS, single-rate and multirate systems can be combined in series or in feedback loops just as in classical control.[4] It has also been shown that a single-rate/multirate system will be stable whenever its ESRS is stable.[7]

The ESRS of a multirate system can be obtained by modeling the multirate system as a periodically time-varying system,[8,9] and transforming the periodically time-varying system into an ESRS.[3] The state-space representation of the ESRS is

$$x(m+1, 0) = A_E x(m, 0) + B_E u_E(m, 0) \tag{1a}$$

$$y_E(m, 0) = C_E x(m, 0) + D_E u_E(m, 0) \tag{1b}$$

where

$$y_E(m, 0) = \begin{bmatrix} y(m, 0) \\ y(m, 1) \\ \vdots \\ y(m, N-1) \end{bmatrix} \quad u_E(m, 0) = \begin{bmatrix} u(m, 0) \\ u(m, 1) \\ \vdots \\ u(m, N-1) \end{bmatrix} \tag{2}$$

for $m = 0, 1, 2, \ldots$, and $n = 0, 1, 2, \ldots, N-1$.

In these equations, $u(m, n)$ and $y(m, n)$ represent the values of the input and output, respectively, of the original multirate system at the $(mN+n)$th sampling instant. The integer N is the ratio of the least common multiple of all of the multirate system's sample/update/delay periods to their greatest common divisor. The subscript E denotes vectors and matrices strictly associated with the ESRS.

A key feature of an ESRS is that its input/output vectors are composite vectors containing the input/output values of the multirate system at N separate sampling times. Consequently, an ESRS is always multiple input, multiple output (MIMO) even if the original multirate system is single input, single output (SISO). Another key feature is that an ESRS always has a nonzero direct feed through term D_E. This is because D_E contains information about how past inputs affect the current output. For systems with no dynamics, the direct feed through term D_E is block diagonal. For example, the ESRS of a constant uncertainty matrix Δ is

$$\Delta_E = \text{block diag}[\Delta, \Delta, \ldots, \Delta] \tag{3}$$

with N blocks.

Refer to Refs. 3, 6, 8, and 9 for the details on modeling a multirate system as an ESRS.

Result 2

A discrete signal $w(m, n)$ is related to its ESRS signal $w_E(m, 0)$ as follows:

$$w(m, n) = [W_N(n)\, W_N(n-1) \cdots W_N(n-N+1)] w_E(m, 0)$$

where $W_N(n)$ is a switching function defined as

$$W_N(k) = \frac{1}{N} \sum_{i=0}^{N-1} \cos\left(\frac{2\pi}{N} ik\right) \tag{4a}$$

Received July 29, 1991; presented as Paper 91-2812 at the AIAA Guidance, Navigation, and Control Conference, New Orleans, LA, Aug. 12–14, 1991; revision received Oct. 22, 1992; accepted for publication Oct. 22, 1992.

*Post Doctoral Researcher, Mechanical Engineering Department.
†Assistant Professor, Mechanical Engineering Department. Member AIAA.

so that

$$W_N(k) = 1 \quad \text{if } k = \pm mN \quad \text{for } m = 0, 1, \ldots$$
$$= 0 \quad \text{otherwise} \tag{4b}$$

Result 2 provides a convenient mathematical connection between the input/output vectors of a multirate system and its ESRS. The form of W_N given in Eq. (4a) is useful for analytic results whereas that given in Eq. (4b) is convenient for numerical simulation.

Result 2 allows one to use single-rate analysis techniques to obtain results for multirate systems. For example, to compute the time domain response of a multirate system to a generic input, we can find the time domain response of the ESRS using any applicable single-rate technique, and then transform that response back to the original multirate system using result 2.

Result 3

The two-norm and rms value of a discrete signal $w(m, n)$ and its ESRS signal $w_E(m, 0)$ are equal or, equivalently,

$$\|w(m, n)\|_2 = \|w_E(m, 0)\|_2 \quad \text{and} \quad \text{rms}[w(m, n)] = \text{rms}[w_E(m, 0)]$$

Result 3 follows directly from Eq. (2) and the definition of the two-norm and rms value.[10]

Result 4

The maximum rms gain of a multirate system is given by the H-infinity norm of its ESRS transfer function $G_E(z)$ or, equivalently,

$$\sup_{\text{rms}\,(u)\neq 0} \frac{\text{rms}\,[y(m, n)]}{\text{rms}\,[u(m, n)]} = \|G_E(z)\|_\infty$$

It is well known that the maximum rms gain of a SISO single-rate system is equivalent to the maximum gain on that system's Bode plot. Although a transfer function for a multirate system does not exist in the traditional sense, we can see from result 4 that the H-infinity norm of a SISO multirate system plays the same role as the maximum Bode plot gain of a single-rate system.

Result 4 follows from result 3 and Refs. 10–12. It is also derived, in part, in Ref. 4.

Result 5

The singular values of a single-rate transfer function $G(z)$ and its ESRS transfer function $G_E(z)$ are related as follows:

$$\sigma[G_E(e^{jN\theta})] = \{\sigma[G(e^{j\theta})]^T\, \sigma[G(e^{j[\theta+(2\pi/N)]})]^T$$
$$\sigma[G(e^{j[\theta+(4\pi/N)]})]^T \cdots \sigma[G(e^{j[\theta+[2\pi(N-1)/N]]})]^T\}^T$$

where $\sigma[\cdot]$ denotes a column vector of singular values.

Result 5 relates the singular values of a single-rate system to the singular values of its ESRS and provides some insight into the significance of the singular values associated with the ESRS of a multirate system. From result 5 we can see that one effect of transforming $G(z)$ into $G_E(z)$ is that the singular values of $G(z)$ at high frequencies are aliased into $G_E(z)$ at lower frequencies. Consequently, the $u(m, n)$ in result 4 that results in the maximum rms gain does not necessarily contain the frequency ω associated with $\|G_E(e^{j\omega T})\|_\infty$ (T is the sampling period of the ESRS). The input signal of maximum rms gain must be constructed using the right singular vectors of $G_E(z)$ and result 2. We will demonstrate this procedure in the following section. (See the Appendix for a derivation of result 5.)

Result 6

The stability, gain margin, and phase margin of a SISO multirate system can be determined directly from a Nyquist plot of its ESRS. Recall from result 1 that the ESRS of a SISO multirate system is MIMO. Therefore, the multiloop Nyquist stability criterion must be used in result 6.[13] This, however, is one case where gain and phase margins taken from a multiloop Nyquist plot can be interpreted in the traditional sense because gain and phase variations at the multirate system's input/output apply simultaneously to all the inputs/outputs of the ESRS.

Result 6 follows from Eq. (3) and is derived in Ref. 1.

Result 7

The robustness of a multirate system can be determined by applying structured and unstructured singular value analysis to that system's ESRS. Given the ESRS transfer function G_E of the nominal system and the uncertainty transfer function Δ_E, we can apply established singular value analysis techniques to find the size of the smallest uncertainty $\bar{\sigma}(\Delta_E)$ that destabilizes the closed-loop system in Fig. 1. This result, however, is only a conservative estimate of the size of the actual smallest destabilizing uncertainty Δ. The input/output vectors of an ESRS are composite vectors, containing the input/output values of the multirate system at N sample times. Thus $\bar{\sigma}(\Delta_E)$ found using unstructured singular value analysis accounts for not only the fictitious perturbations normally associated with unstructured singular values, but also for time-varying and noncausal perturbations. A valid perturbation for a given $\bar{\sigma}(\Delta_E)$ might, for example, include block diagonal elements in Δ_E that are unequal. This corresponds to a time-varying perturbation because the gain between $u(m, n)$ and $y(m, n)$ varies with n. Another valid perturbation could include nonzero upper block diagonal elements in Δ_E. This corresponds to a noncausal perturbation because a future input $u(m, n+1)$ can affect the current output $y(m, n)$.

For the ESRS uncertainty Δ_E to represent the actual uncertainty Δ, its structure must obey Eq. (1). Finding $\bar{\sigma}(\Delta_E)$ subject to Eq. (1) requires the solution of a structured singular value problem. Unfortunately, even simply structured dynamic uncertainties in a single-rate/multirate system transform to uncertainties with complex structures in the ESRS. The complex structure makes it difficult to obtain a good estimate of the size of the smallest destabilizing structured perturbation. However, when the single-rate/multirate uncertainty is a constant, as is the case for many problems, the ESRS uncertainty is also a constant with a repeated block diagonal form [see Eq. (3)]. A good estimate of the solution of such a structured singular value problem with repeated blocks can be found using one of the methods in Refs. 14–17.

Result 7 follows directly from the fact that a single-rate/multirate system is stable if and only if its ESRS is stable.[7]

Application

In this section we apply the results of the previous section to a real world example: a multirate flutter suppression system for a model wing. This application points out some of the practicalities of multirate robustness analysis.

The model wing used in this example is being developed under the Benchmark Active Controls Project at the NASA Langley Research Center. It consists of a rigid airfoil mounted on a pitch and plunge apparatus (PAPA). The PAPA mount provides the two degrees of freedom needed to model classical wing flutter. The wing has one control surface located on the trailing edge (TE) of the airfoil. Two accelerometers measure pitch and plunge accelerations. We used a 15th-order mathematical model of the wing for the control system design. This model incorporates a second-order Dryden gust filter, a third-order actuator model, and a 10th-order

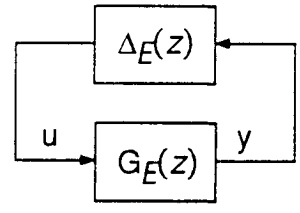

Fig. 1 ESRS $G_E(z)$ with factored uncertainty $\Delta_E(z)$.

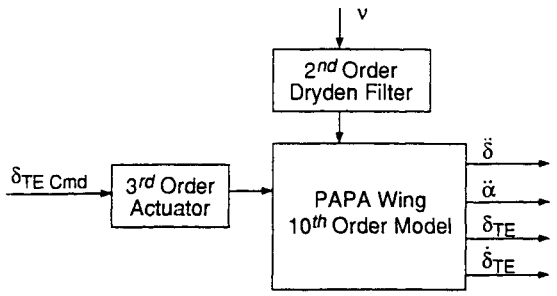

$\delta_{TE\,Cmd}$ = TE Control Surface Command Input
$\ddot{\delta}$ = Plunge Acceleration
$\ddot{\alpha}$ = Pitch Acceleration
δ_{TE} = Control Surface Deflection
$\dot{\delta}_{TE}$ = Control Surface Deflection Rate
v = Disturbance Input

Fig. 2 Block diagram of model wing with pitch and plunge apparatus.

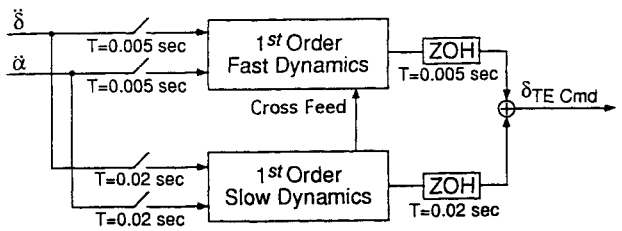

Fig. 3 Block diagram of the second-order multirate compensator.

airfoil model (two rigid body modes and six unsteady aero states). A block diagram of this model is shown in Fig. 2.

A second-order multirate flutter suppression system was designed for the model wing. The multirate compensator, shown in Fig. 3, consists of two first-order control loops. The slow loop is sampled/updated at 50 Hz. The fast loop is sampled/updated at 200 Hz, resulting in $N = 4$. We optimized all of the free parameters in this compensator using the multirate compensator synthesis algorithm described in Ref. 9. The free parameters were the pole and zero locations for the fast and slow loops, the gain values for the fast and slow loops, and gain values for the cross feed between the fast and slow loops.

To analyze the robustness of the closed-loop system we examined the gain and phase margins at the plant input and output and the rms gains from disturbance input to the control surface deflection and deflection rate. Gain and phase margins provide a measure of the uncertainty allowed in the plant model. The rms gains provide a measure of the allowable disturbance level before the control surface actuator limits are exceeded.

Traditional gain and phase margins at the plant input were calculated using result 6. The location of the corresponding complex loop gain k_u is shown in Fig. 4. The multiloop Nyquist diagram for the open-loop ESRS is shown in Fig. 5. Gain and phase margins calculated from the Nyquist diagram are given in Table 1.

Generalized gain and phase margins at the plant output were calculated using the ESRS and the structured singular value. For this analysis, the closed-loop system was cast into the form of the block diagram shown in Fig. 1. The uncertainty block Δ and the corresponding Δ_E are

$$\Delta = \begin{bmatrix} k_1 & 0 \\ 0 & k_1 \end{bmatrix} \qquad \Delta_E = \begin{bmatrix} I_N k_1 & 0 \\ 0 & I_N k_2 \end{bmatrix} \tag{5}$$

where I_N is an $N \times N$ identity matrix. The complex gain uncertainties k_1 and k_2 represent additive plant output uncertainties. They are shown in Fig. 4. G_E (in Fig. 1) is the nominal closed-loop system comprised of the model wing and the multirate flutter suppression system.

The form of the uncertainty Δ_E in Eq. (5) leads directly to a structured singular value problem with repeated scalar block uncertainties. Typically, an exact solution for such a problem is difficult to find. Fortunately, this problem has only two free parameters, k_1 and k_2, and an exact solution can be found. We calculated an exact value of the size of the smallest destabilizing uncertainty using the following equation[14]:

$$\frac{1}{\bar{\sigma}(\Delta_{\min})} = \sup_{0<\phi<\pi} \max_{0<\theta<2\pi} \rho\{U(\theta)\, G_E(e^{j\phi})\} \tag{6}$$

with

$$U(\theta) = \begin{bmatrix} I & 0 \\ 0 & e^{j\theta} I \end{bmatrix}$$

where $\bar{\sigma}(\Delta_{\min})$ is the maximum singular value of the smallest destabilizing Δ; and $\rho(\cdot)$ is the spectral radius. The resulting value of $\bar{\sigma}(\Delta_{\min})$ is given in Table 1.

Generalized gain and phase margins corresponding to $\bar{\sigma}(\Delta_{\min})$ were calculated using the method described in Ref. 18. Figure 6 shows the "region of guaranteed stability" for simultaneous (independent) gain and phase changes in $1+k_1$ and $1+k_2$.

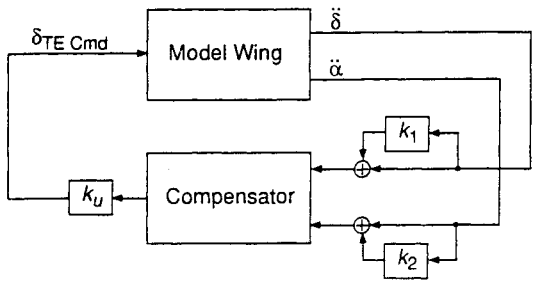

Fig. 4 Location of the complex gains used for gain and phase margin analysis; nominal system: $k_u=1$, $k_1=k_2=0$.

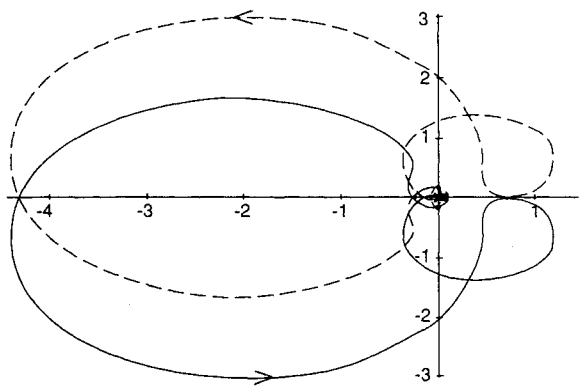

Fig. 5 Multiloop Nyquist plot of PAPA wing with multirate compensator; the control loop is broken at k_u with $k_1=k_2=0$; open-loop system has two unstable poles.

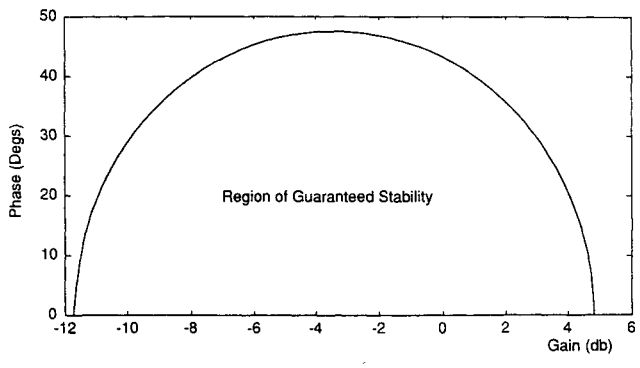

Fig. 6 Region of guaranteed stability for simultaneous changes in the gain and phase of $(1+k_1)$ and $(1+k_2)$.

Table 1 Robustness results for multirate flutter suppression system

Gain margin at plant input (with $k_1=k_2=0$), dB	$[-12, +10]$
Phase margin at plant input (with $k_1=k_2=0$), deg	± 65
$\bar{\sigma}(\Delta_{\min})$ with $k_u=1$	0.74
Maximum rms gain, v to δ_{TE}, deg·s/in.	0.125
Maximum rms gain, v to $\dot{\delta}_{TE}$, deg/in.	4.67

The maximum rms gain values for disturbance input to control surface deflection and deflection rate were calculated using result 4. Result 4, however, is directly applicable only to discrete systems and not to our mixed continuous/discrete system. Therefore, we discretized the plant disturbance input and control surface deflection and deflection rate outputs at 500 Hz, assuming a zero-order hold at the disturbance input. This sampling rate is 30 times the Dryden filter roll-off frequency. The values of the maximum rms gains are then the peak values of the maximum singular value plots of this new multirate system (see Fig. 7). The peak values, which occur at $\omega_{max}=27$ rad/s, are given in Table 1. Since we assumed a stair step disturbance input, the values in Table 1 are lower, yet very close, bounds on the maximum rms gains.[19]

Contrary to what occurs in linear time invariant single-rate systems, we cannot assume that the signal producing the maximum rms gain $u_{\max\,rms}(m, n)$ has the simple form $\sin(w_{max}Tm)$. Instead, we must construct $u_{\max\,rms}(m, n)$ using result 2. For our example, the input signal of maximum rms gain $u_{\max\,rms}(m, n)$ from the disturbance v to the control surface deflection δ_{TE} was found as follows. Let

$$G_E(e^{j\omega_{max}T})=\text{transfer function from } v \text{ to } \delta_{TE} \text{ evaluated at } \omega_{max} \tag{7a}$$

and

$$\begin{bmatrix} \alpha_1 e^{j\phi_1} \\ \alpha_2 e^{j\phi_2} \\ \vdots \\ \alpha_N e^{j\phi_N} \end{bmatrix} = \text{right singular vector associated with } \sigma\,[G_E(e^{j\omega_{max}T})] \tag{7b}$$

Then, $u_{\max\,rms}(m, n)$ is given by

$$u_{\max\,rms}(m, n) = [W_N(n)\, W_N(n-1) \cdots W_N(n-N+1)] \times \begin{bmatrix} \alpha_1 \sin(\omega_{max}Tm+\phi_1) \\ \alpha_2 \sin(\omega_{max}Tm+\phi_2) \\ \vdots \\ \alpha_N \sin(\omega_{max}Tm+\phi_N) \end{bmatrix} \tag{8}$$

where W_N is the switching function described in result 2, and T is the sampling period of the ESRS.

From Eqs. (4) and (8) it is straightforward to see that, in general, the signal of maximum rms gain for a multirate system is comprised of the sum of sinusoids of several distinct frequencies. In this example, though, $u_{\max\,rms}(m, n)$ is comprised almost purely of a single sinusoid of frequency of 27 rad/s. This is because higher frequency signals which might interact with the multirate compensator and increase the rms gain are attenuated by the Dryden filter and plant dynamics.

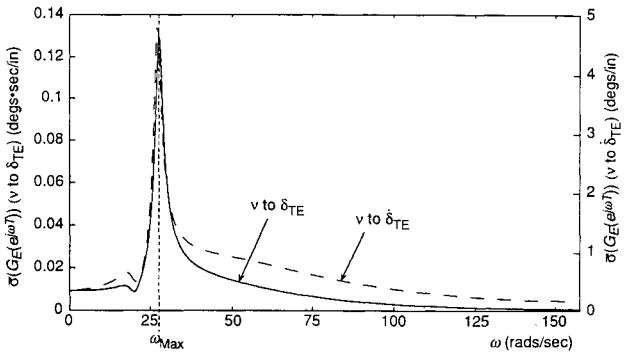

Fig. 7 Maximum singular value plots of v to δ_{TE} and v to $\dot{\delta}_{TE}$, =0.02 s.

Conclusions

In this paper we have summarized some important multirate robustness analysis results. The foundation for these results is the equivalent single-rate system. This system allows one to analyze the stability and robustness of a multirate system using well-known single-rate techniques.

There are, however, drawbacks to using the equivalent single-rate system. First, the composite structure of its inputs and outputs leads to matrix transfer functions of high order. This is a problem especially when the ratio of the longest to the shortest sampling/update/delay period of the multirate system is large. Second, even when the simplest constant parameter uncertainty model is used for robustness analysis, the composite input and output structure gives rise to a structured singular value problem with repeated diagonal blocks. This is a numerically difficult problem to solve.

In short, multirate system stability and robustness analysis based on the equivalent single-rate system is straightforward because the analysis can be performed using established single-rate techniques, but the results must be interpreted carefully in accordance with its input/output structure.

Appendix

Lemma:

$$\sigma[G_E(e^{jN\theta})]=\{\sigma[G(e^{j\theta})]^T\,\sigma[G(e^{j[\theta+2\pi/N]})]^T \sigma[G(e^{j(\theta+4\pi/N)})]^T \cdots \sigma[G(e^{j[\theta+[2\pi(N-1)/N]]})]^T\}^T$$

Proof: Let $G(z)$ and $G_E(z^N)$ be the transfer functions of a single-rate system and its ESRS, respectively, such that

$$y(z) = G(z)u(z) \qquad \text{and} \qquad y_E(z^N) = G_E(z^N)u_E(z^N) \tag{A1}$$

We have written $G_E(z^N)$ as a function of z^N because the sampling period for the ESRS is N times that of the single-rate system associated with $G(z)$.

It is shown in Ref. 3 that

$$y(z) = [I \;\; z^{-1}I \;\; z^{-2}I \;\cdots\; z^{-N-1}I\,]\, y_E(z^N) \tag{A2}$$

where I is an identity matrix of appropriate dimensions.

Now define

$$\tilde{y}(z) = \begin{bmatrix} y(\phi^0 z) \\ y(\phi^1 z) \\ \vdots \\ y(\phi^{N-1} z) \end{bmatrix}, \qquad \tilde{u}(z) = \begin{bmatrix} u(\phi^0 z) \\ u(\phi^1 z) \\ \vdots \\ u(\phi^{N-1} z) \end{bmatrix} \tag{A3}$$

and

$$\tilde{G}(z)=\text{block diag}[G(\phi^0 z), G(\phi^1 z), \ldots, G(\phi^{N-1} z)] \tag{A4}$$

where

$$\phi = e^{(2\pi j/N)}$$

such that

$$\tilde{y}(z) = \tilde{G}(z)\tilde{u}(z) \tag{A5}$$

We can now write $\tilde{y}(z)$ and $\tilde{u}(z)$ in terms of $y_E(z^N)$ and $u_E(z^N)$ using Eq. (A2).

$$\tilde{y}(z) = T(z)y_E(z^N) \qquad \tilde{u}(z) = T(z)u_E(z^N) \tag{A6}$$

where

$$T(z) = \begin{bmatrix} I & z^{-1}I & \cdots & z^{-(N-1)}I \\ I & (\phi^1 z)^{-1}I & & (\phi^1 z)^{-(N-1)}I \\ & \vdots & & \vdots \\ I & (\phi^{N-1} z)^{-1}I & \cdots & (\phi^{N-1} z)^{-(N-1)}I \end{bmatrix} \tag{A7}$$

Then from Eqs. (A1) and (A5) through (A6)

$$G_E(z^N) = T^{-1}\tilde{G}(z)T \tag{A8}$$

Noticing that $T(e^{j\theta})T(e^{j\theta})^* = NI$, we can define a unitary matrix $\tilde{T}(e^{j\theta})$ such that

$$T(e^{j\theta}) = \sqrt{N}\tilde{T}(e^{j\theta}) \qquad \text{and} \qquad T(e^{j\theta})^{-1} = (1/\sqrt{N})\tilde{T}(e^{j\theta})^* \tag{A9}$$

Now, using Eqs. (A8) and (A9) and the properties of unitary matrices, it is straightforward to show that

$$\sigma[G_E(e^{jN\theta})] = \sigma[\tilde{G}(e^{jN\theta})] \tag{A10}$$

Since $\tilde{G}$ is block diagonal [see Eq. (A4)], and the singular values of a block diagonal matrix are the union of the singular values of each block, we can rewrite Eq. (A10) as follows:

$$\sigma[G_E(e^{jN\theta})] = \{\sigma[G(e^{j\theta})]^T \ \sigma[G(e^{j[\theta+(2\pi/N)]})]^T$$

$$\sigma[G(e^{j[\theta+(4\pi/N)]})]^T \cdots \sigma[G(e^{j[\theta+[2\pi(N-1)/N]]})]^T\}^T$$

Acknowledgment

This research was supported by NASA Langley Research Grants NCC1-156 and NAG-1-1055.

References

[1]Thompson, P. M., "Gain and Phase Margins of Multirate Sampled-Data Feedback Systems," *International Journal of Control*, Vol. 44, No. 3, 1986, pp. 833–846.

[2]Thompson, P. M., and Dailey, R. L., "Kranc Vector Switch Decomposition in State Space," Caltech Internal Rept., California Inst. of Technology, Davis, CA, Sept. 1985.

[3]Meyer, R. A., and Burrus, C. S., "A Unified Analysis of Multirate and Periodically Time-Varying Digital Filters," *IEEE Transactions on Circuits in Systems*, Vol. CAS-22, No. 3, March 1975, pp. 162–168.

[4]Khargonekar, P. P., Poolla, K., and Tannenbaum, A., "Robust Control of Linear Time-Invariant Plants Using Periodic Compensators," *IEEE Transactions on Automatic Control*, Vol. AC-30, No. 11, Nov. 1985, pp. 1088–1096.

[5]Boykin, W. H., and Frazier, B. D., "Multirate Sampled-Data Systems Analysis Via Vector Operators," *IEEE Transactions on Automatic Control*, Vol. AC-20, No. 4, Aug. 1975, pp. 548–551.

[6]Apostolakis, I. S., and Jordan, D., "Multirate System Performance Evaluation Using Singular Value Analysis," *Proceedings of the 1990 American Control Conference*, IEEE, Piscataway, NJ, 1990, pp. 1502–1507.

[7]Kono, M., "Eigenvalue Assignment in Linear Periodic Discrete-Time Systems," *International Journal of Control*, Vol. 32, No. 1, 1980, pp. 149–158.

[8]Berg, M. C., Mason, G. S., and Yang, G. S., "A New Multirate Sampled-Data Control Law Structure and Synthesis Algorithm," *Journal of Guidance, Control, and Dynamics*, Vol. 15, No. 5, 1992, pp. 1183–1191.

[9]Mason, G. S., and Berg, M. C., "Reduced Order Multirate Compensator Synthesis," *Journal of Guidance, Control, and Dynamics*, Vol. 15, No. 3, 1992, pp. 700–706.

[10]Boyd, S., and Doyle, J., "Comparison of Peak and RMS Gains for Discrete-Time Systems," *Systems and Control Letters*, Vol. 9, 1987, pp. 1–6.

[11]Maciejowski, J. M., *Multivariable Feedback Design*, Addison-Wesley, Reading, MA, 1990.

[12]Francis, B. A., "A Course in H_∞ Control Theory," *Lecture Notes in Control and Information Sciences*, Vol. 88, Springer-Verlag, New York, 1987.

[13]MacFarlane, A. G. J., "Return-Difference and Return-Ratio Matrices and Their Use in Analysis and Design of Multivariable Feedback Control Systems," *IEE Proceedings on Control Theory and Applications*, Pt. D, Vol. 117, No. 10, Oct. 1970, pp. 2037–2049.

[14]Doyle, J., "Analysis of Feedback Systems with Structured Uncertainties," *IEE Proceedings on Control Theory and Applications*, Pt. D, Vol 129, No. 6, Nov. 1982, pp. 243–250.

[15]Safonov, M.G., "Stability Margins of Diagonally Perturbed Multivariable Feedback Systems," *IEE Proceedings on Control Theory and Applications*, Pt. D, Vol. 129, No. 6, Nov. 1982, pp. 251–256.

[16]Safonov, M., and Doyle, J. C., "Minimizing Conservativeness of Robustness Singular Values," *Multivariable Control: New Concepts and Tools*, D. Reidel, Hingham, MA, 1984, pp. 197–207.

[17]Packard, A., and Doyle, J., "Structured Singular Value with Repeated Scalar Blocks," *Proceedings of the 1988 American Control Conference*, IEEE, Piscataway, NJ, 1988, pp. 1213–1218.

[18]Mukhopadhyay, V., and Newsom, J. R., "Multiloop System Stability Margin Study Using Matrix Singular Values," *Journal of Guidance, Control, and Dynamics*, Vol. 7, No. 5, 1984, pp. 582–587.

[19]Sivashankar, N., and Khargonekar, P. P., "Robust Stability and Performance Analysis of Sampled-Data Systems," *Proceedings of the IEEE Conference on Decision and Control*, IEEE Piscataway, NJ, pp. 881–885.